があった場合，狭い部位に関しては考慮されない点があげられる．また先天奇形を伴った視神経乳頭など分類が困難な視神経乳頭を，評価することは困難である．このシステムは，C/D比に比べてやや複雑であるが，基本的な考え方としては，緑内障を評価する際には，乳頭陥凹の大きさよりもむしろリムの厚みに注目し，視神経乳頭を観察するという原則や，緑内障性変化は小さい乳頭では過少評価され，大きい乳頭では過大評価されやすい点を考慮している点はわれわれが通常診療において常に気をつけている点と一致している．しかし，C/D比にしろDDLSにしろいずれの評価法においても，評価は主観的で観察者に依存する．その点を克服するために，画像解析装置が用いられてきている．

IV 最近の画像解析装置（HRTおよびOCT）

視神経乳頭を定量的に評価して客観的に緑内障を診断し，経過観察を行うための手段として，近年Heidelberg Retina Tomograph（HRT；Heidelberg Engineering, Dossenheim, Germany）と光干渉断層計（Optical Coherence Tomography：OCT；Carl Zeiss Meditec, Dublin, CA）などが用いられてきている（症例呈示：図3a～d）．

1. Heidelberg Retina Tomograph II（HRT II）

HRTは波長670 nmのダイオードレーザーを使用した共焦点レーザー走査型顕微鏡で，優れた測定再現性および乳頭パラメータの信頼性をもつ画像解析装置である．近年HRTの普及型として解析部位を視神経乳頭に絞り，撮影画角のサイズを15°×15°に固定したHRT IIが導入された．

HRT IIでは検査にあたって散瞳する必要はなく，内部固視灯を被検者が固視するとちょうど画面の中央に視神経乳頭が位置するように設定されている．検査眼のフォーカスを合わせて一度操作ボタンを押すだけでHRT IIは自動的にスキャン幅を決定し，その後3回連続して画像を取り込み，面倒な設定なしに短時間で平均画像を得ることができる．取り込んだ画像は16から64枚の連続的で等距離（1/16 mm）の二次元のシリーズ画像で構成され，各二次元画像は384×384ピクセルの解像度をもつ．コンピュータがその画像を立体的に再構築し，三次元解析が可能となる．検者が測定画面上で視神経乳頭縁（コントアライン）を決定すると，自動的にコントアラインに沿った網膜表面の高さが得られる（図

図3 左緑内障眼のステレオ眼底写真（a），HRT II解析結果（b），OCT 3のOptic Nerve Head解析画面（c）およびHumphrey視野（d）

a：乳頭陥凹は拡大しており，5時から6時のリムは完全に消失している（白両矢印）．明瞭ではないが，2時と5時に網膜神経線維層欠損（NFLD）（黒矢印で囲まれた部位）がみられる．

b：ベースライン検査では，トポグラフィ画像（**上段左**），反射画像（**上段右**），Y軸高さプロファイル（**上段中央**），X軸高さプロファイル（**中段左**），コントアラインの高さ変化（**中段右**），立体計測パラメータ（**下段左**）およびMoorfields回帰解析結果（**下段右**）が表示される．トポグラフィ画像は，各測定点における眼底表面の高さを表している．明部は凹部，暗部は凸部を表している．さらに乳頭には赤/青/緑のオーバーレイを表示．赤の領域は視神経乳頭の陥凹領域で，乳頭の残りのリム領域は，傾斜部（青）と平らな部分（緑）に分けられる．反射画像は，各測定点の反射率を表示．明るい部分はより多くの反射光がカメラに戻ってきた場所を示す．さらに視神経乳頭を6分割して各セクターのMoorfields回帰解析判定結果を重ねて表示．Moorfields回帰解析判定が“within normal limits”，“borderline”，“outside normal limits”であれば，それぞれ緑色のチェックマーク，黄色の感嘆符，赤い×印が表示される．コントアラインの高さは耳側，上側，鼻側，下側の順に展開した曲線として表示（**中段右**）．この症例ではMoorfields回帰解析は“Outside normal limits”（**下段右**）．HRT IIで測定した視神経乳頭サイズ（Disk Area）2.234 mm^2，垂直C/D比（Linear Cup/Disk Ratio）は0.792（**下段左**）．

c：画面左にスキャン画像（この図では垂直方向のスキャン），その下に眼底画像が表示される．スキャン画像中のライトブルーの円内のライトブルーの2本の直線の交点（白矢印）が網膜色素上皮の終結する参照点．この2点の参照点間を結んだ直線が乳頭径と定義される．この直線に対して150 μm前方に平行する赤点線（赤矢印）より高い位置がリム（赤の凝縮された部位），低い位置が陥凹とされる．画面右側の表示は視神経乳頭解析画像で，6本の放射状スキャン画像から構築される視神経乳頭の合成画像．赤線で囲まれた円の内部がDisk Area，緑線で囲まれた円の内部がCup Area．OCT 3で測定した視神経乳頭サイズ（Disk Area）2.394 mm^2，垂直C/D比（Cup/Disk Vert. Ratio）は0.885（**下段右**）．

d：Humphrey視野では，下方のリム消失に対応した上方の視野変化および2時のNFLDに対応すると思われる下方の視野変化（グレースケールでは，はっきりしないが，パターン偏差では明瞭となっている）がみられる．HfaFiles Ver5（Beeline Office Co. Japan）によるプリントアウト．

3b 中段右)．耳側 350°～356°のセクターにみられる乳頭黄斑束部のコントアラインの平均の高さより 50 μm 低い位置は，神経線維層の底の部分とほぼ同じ位置になり，その線がリファレンスプレーンの位置となる．リファレンスプレーンより上がリム，リファレンスプレーンより下が陥凹と定義される．

HRT II では視神経乳頭に関する多くのパラメータが表示されるとともに，視神経乳頭の緑内障性変化の有無を判定する自動診断プログラムが付属されている．視神経乳頭を 6 セクターに分け，Wollstein ら[6] が報告した Moorfields の回帰解析に基づき全体と各セクターでのリム面積と乳頭領域の面積比を評価することにより，"within normal limits"，"borderline"，"outside normal limits" の 3 段階で判定する (図 3b の下段右)．

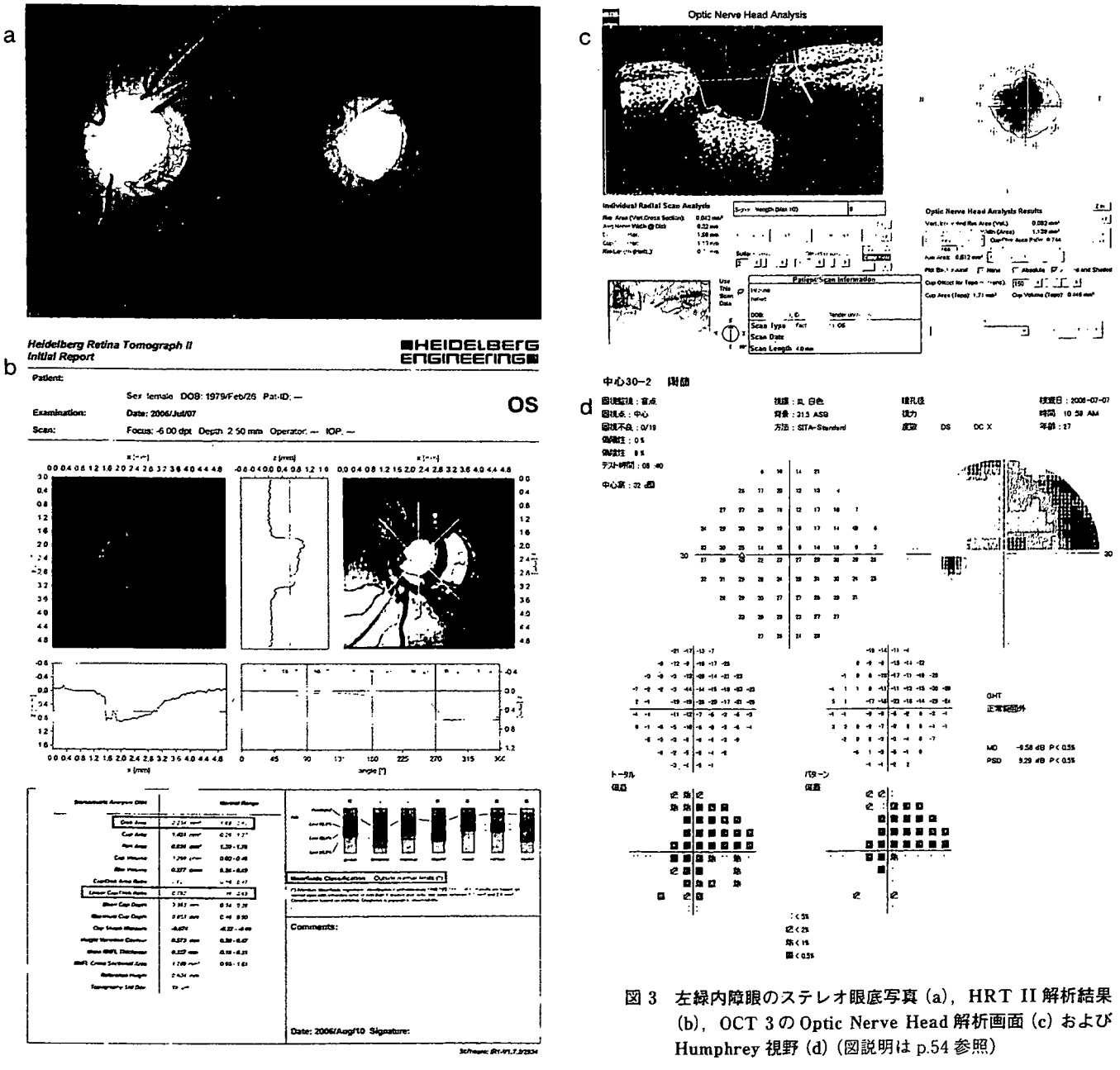

図 3　左緑内障眼のステレオ眼底写真 (a)，HRT II 解析結果 (b)，OCT 3 の Optic Nerve Head 解析画面 (c) および Humphrey 視野 (d) (図説明は p.54 参照)

2. Optical Coherence Tomography 3000 (OCT 3)

近年OCTも，緑内障診断に用いられている．OCTは従来の超音波を用いた画像診断と類似の原理に基づく測定機器であり，超音波の代わりにダイオード光源による波長820nmの近赤外線低干渉光を用いるため，非侵襲的に高い解像度の画像が得られ，OCT 3では縦断面，横断面ともに10μmの解像度が得られる．OCT 3では，検査可能な被検者の最小瞳孔径が3.2mmとなったので，無散瞳でも検査可能になった．

OCT 3には，緑内障診断補助プログラムとして，RNFL Thickness Average（網膜神経線維層厚解析），RNFL Thickness Map（網膜神経線維層厚マップ），Optic Nerve Head Analysis（視神経乳頭解析）がある．

そのなかで乳頭解析プログラムとしてはOptic Nerve Head Analysis（視神経乳頭解析）があり，視神経乳頭を4mmの放射状ラインで6本スキャンして得られる結果から，水平・垂直C/D比，リム面積・体積，カップ径，陥凹の深さなどが自動的に計測解析される（図3c）．この解析では反射輝度の特定の閾値を検索することによって神経線維層前面と網膜色素上皮を検出する．解剖学的に網膜色素上皮が終結する視神経乳頭の両端が解剖学的マーカー（参照点）として決定され，この2点が視神経乳頭の全解析の基本となる．視神経乳頭両端の2点の参照点間を直線で結ぶことにより乳頭径が求められる．この直線に対して150μm前方に平行する赤点線より高い位置がリム，低い位置が陥凹とされる．これらは客観的に自動的に計算されるが，手動で参照点を調整することができる．

OCT 3では，解像度は低いが6本のラインスキャンを1.92秒で一度に捉えることができるfast scansというシステムが導入された．通常の高解像度のスキャンでは1本のラインのスキャンに1.28秒かかり，これを少なくとも6本測定しなければならない．Kamppeterら[7]は，正常人を通常のモード（Optical Disc），fast scansモード（Fast Optical Disc）の2つのモードで測定し，それぞれにおいて自動で参照点を決めて計算した場合と，参照点を手動で修正した場合で再現性について検討し，通常のモードで修正しなかった場合はアーチファクトのため良いデータが得られず，fast scansモードで参照点を手動で修正した場合が最も再現性が高かったと報告している．その理由として，1本ずつ捉えるパターンでは全スキャンが終了するまで時間がかかり，その間患者の固視移動，スキャン部位の移動などで解析結果にばらつきが生じるためと思われる．

3. HRT IIとOCT 3の測定値の比較（図3）

近年それぞれの測定値の関係について検討されてきている．HRT IIとOCT 3で測定した視神経乳頭面積は高い相関があるが，HRT IIで測定した平均の視神経乳頭面積は，OCTで測定した乳頭面積よりいずれの視神経乳頭サイズでも常に小さい傾向にあるようだ[8,9]．Arthurら[10]は，水平C/D比と垂直C/D比について，同時撮影ステレオ眼底写真，HRT II，OCT 3で比較し，OCT 3が水平C/D比と垂直C/D比ともに最も大きく，水平C/D比が最も小さかったのは同時撮影ステレオ眼底写真で，垂直C/D比が最も小さかったのはHRT IIであったと報告している．水平C/D比と垂直C/D比ともにOCTは陥凹の最長径に対する視神経乳頭最長径の比率を計算しているのに対して，HRT IIでは視神経乳頭の中心でC/D比を測定している．この点が，OCTのC/D比が，HRT IIのC/D比より大きい理由の一つと考察されている．各機器で測定された各パラメータはそれぞれよく相関しているが，それぞれの機器のデータの互換性は今のところないので，同一機種間での経過観察には使用できるが，各パラメータを比較する際には注意を要する．

おわりに

いかに画像解析装置が進歩しようとも，視神経乳頭を立体的に観察することは緑内障診療の基本であり，視神経乳頭を常に立体的に観察する習慣をつける必要がある．C/D比なり，DDLSなり自分なりの視神経乳頭変化の定量化システムをもつことは，緑内障の診断，病期分類および経過観察の際に重宝する．最新の画像解析装置は再現性も信頼性も高く，客観的に定量化することができ，診断および経過観察の心強い補助診断機器と思われる．

文　献

1) Iwase A, Suzuki Y, Araie M et al : The prevalence of primary open-angle glaucoma in Japanese. *Ophthalmology* **111** : 1641-1648, 2004
2) Armaly MF : The optic cup in the normal eye. I. Cup width, depth, vessel displacement, ocular tension and outflow facility. *Am J Ophthalmol* **68** : 401-407, 1969
3) Caprioli J, Miller JM : Videographic measurements of optic nerve topography in glaucoma. *Invest Ophthalmol Vis Sci* **29** : 1294-1298, 1988
4) Bayer A, Harasymowycz P, Henderer JD et al : Validity of a new disk grading scale for estimating glaucomatous damage : correlation with visual field damage. *Am J Ophthalmol* **133** : 758-763, 2002
5) Spaeth GL, Lopes JF, Junk AK et al : System for staging the amount of optic nerve damage in glaucoma : a criteria review and new material. *Surv Ophthalmol* **51** : 293-315, 2006
6) Wollstein G, Garway-Heath DF, Hitchings RA : Identification of early glaucoma cases with the scanning laser ophthalmoscope. *Ophthalmology* **105** : 1557-1563, 1998
7) Kamppeter BA, Schubert KV, Budde WM et al : Optical coherence tomography of the optic nerve head : interindividual reproducibility. *J Glaucoma* **15** : 248-254, 2006
8) Hoffmann EM, Bowd C, Medeiros FA et al : Agreement among 3 optical imaging methods for the assessment of optic disc topography. *Ophthalmology* **112** : 2149-2156, 2005
9) Schuman JS, Wollstein G, Farra T et al : Comparison of optic nerve head measurements obtained by optical coherence tomography and confocal scanning laser ophthalmoscopy. *Am J Ophthalmol* **135** : 504-512, 2003
10) Arthur SN, Aldridge AJ, De Leon-Ortega J et al : Agreement in assessing cup-to-disc ratio measurement among stereoscopic optic nerve head photographs, HRT II, and Stratus OCT. *J Glaucoma* **15** : 183-189, 2006

Ocular Amyloid Angiopathy Associated with Familial Amyloidotic Polyneuropathy Caused by Amyloidogenic Transthyretin Y114C

Takahiro Kawaji, MD,[1] Yukio Ando, MD, PhD,[2] Masaaki Nakamura, MD, PhD,[2] Taro Yamashita, MD, PhD,[2] Miki Wakita, MD,[1] Eiko Ando, MD, PhD,[1] Akira Hirata, MD, PhD,[1] Hidenobu Tanihara, MD, PhD[1]

Purpose: To report the clinicopathological findings for a unique ocular amyloid angiopathy in patients with familial amyloidotic polyneuropathy (FAP) caused by amyloidogenic transthyretin Y114C.

Design: Three case reports.

Methods: Retrospective review of clinicopathological findings, course, and treatment of the 3 patients.

Main Outcome Measures: Visual acuity, intraocular pressure, fundus photography, fluorescein angiography (FA), indocyanine green angiography, and histopathological analysis.

Results: In the 32-year-old patient, in the early stage of FAP, indocyanine green angiography demonstrated multiple sites of hyperfluorescence, with staining along major choroidal veins. Retinal vessels appeared normal clinically and on FA. In the 48-year-old patient, who had late-stage FAP, examination of the fundus revealed pinpoint white amyloid opacities over the retinal surface, sheathing of retinal vessels, and scattered retinal hemorrhages. Fluorescein angiography showed vascular closure, focal staining, and microaneurysms. Indocyanine green angiography revealed multiple sites of hyperfluorescence, with staining along retinal and choroidal vessels. Examination during follow-up revealed that these vascular changes continued to progress. Histopathological study of an eye obtained at autopsy from the 49-year-old patient revealed marked intravascular and extravascular amyloid deposition.

Conclusions: Severe and progressive amyloid angiopathy causing visual disturbance was seen in patients with FAP caused by amyloidogenic transthyretin Y114C. *Ophthalmology 2005;112:2212–2218 © 2005 by the American Academy of Ophthalmology.*

Cerebral amyloid angiopathy (CAA) has been the focus of recent attention during studies of several types of amyloidosis, such as Aβ and cystatin C amyloidoses,[1,2] and transthyretin-related familial amyloidotic polyneuropathy (FAP).[3–7] Cerebral amyloid angiopathy is one of the clinicopathological entities that demonstrate the deposition of amyloid within walls of cerebral vessels.[1] Although the anatomical structures of vessels in the eye are similar to those in the central nervous system (CNS), amyloid angiopathy has never been fully evaluated in the eye.

Familial amyloidotic polyneuropathy, a disorder inherited in an autosomal dominant fashion, is characterized by systemic accumulation of polymerized mutated amyloidogenic transthyretin in peripheral nerves and in organs.[8,9] More than 100 point mutations, most of which lead to production of amyloidogenic transthyretin, have been identified in patients with FAP.[10] Of these amyloidogenic transthyretin mutations, amyloidogenic transthyretin V30M is the most common. In FAP amyloidogenic transthyretin V30M, common ocular manifestations that occur during the course of the illness include abnormal conjunctival vessels, lacrimal dysfunction, pupillary disorders, vitreous opacity, and glaucoma,[11–16] but retinal and choroidal vascular lesions are rare. In FAP induced by some of the

Originally received: March 1, 2005.
Accepted: May 29, 2005. Manuscript no. 2005-180.

[1] Department of Ophthalmology and Visual Science, Graduate School of Medical Sciences, Kumamoto University, Kumamoto, Japan.

[2] Department of Diagnostic Medicine, Graduate School of Medical Sciences, Kumamoto University, Kumamoto, Japan.

Presented at: Association for Research in Vision and Ophthalmology annual meeting, May, 2005; Fort Lauderdale, Florida.

The authors' work was supported by grants from the Amyloidosis Research Committee, Tokyo, Japan; Pathogenesis, Therapy of Hereditary Neuropathy Research Committee, Tokyo, Japan; Surveys and Research on Specific Disease, Tokyo, Japan; Ministry of Health and Welfare, Tokyo, Japan; Charitable Trust Clinical Pathology Research Foundation of Japan, Tokyo, Japan; and Ministry of Education, Science, Sports and Culture, Tokyo, Japan (Grants-in-Aid for Scientific Research).

Correspondence to Yukio Ando, MD, PhD, Department of Diagnostic Medicine, Graduate School of Medical Sciences, Kumamoto University, 1-1-1 Honjo, Kumamoto 860-8556, Japan. E-mail: yukio@kaiju.medic.kumamoto-u.ac.jp.

ISSN 0161-6420/05/$–see front matter
doi:10.1016/j.ophtha.2005.05.028

other types of amyloidogenic transthyretin, in contrast to FAP amyloidogenic transthyretin V30M, amyloid deposition occurs in oculoleptomeninges (ocular tissues, leptomeninges, and cerebral vessel walls), which often leads to ocular manifestations and CNS disorders, with mild polyneuropathy.

Patients with FAP caused by amyloidogenic transthyretin Y114C (a point mutation, from tyrosine to cysteine, at codon 114) have been found in Japan and the Netherlands; they had polyneuropathy, cardiopathy, autonomic dysfunction, and ocular manifestations, which included severe vitreous opacity and glaucoma.[17,18] We recently evaluated 3 patients with FAP caused by amyloidogenic transthyretin Y114C by using indirect fundus examination, fluorescein angiography (FA), indocyanine green angiography, and histopathological analysis, and we report here the clinicopathological findings related to a unique ocular amyloid angiopathy.

Case Reports

The 3 patients, who were from related kindred with FAP caused by amyloidogenic transthyretin Y114C, were referred to Kumamoto University Hospital and underwent ophthalmological and neurological examinations. Table 1 (available at http://aaojournal.org) provides clinical characteristics of the patients.

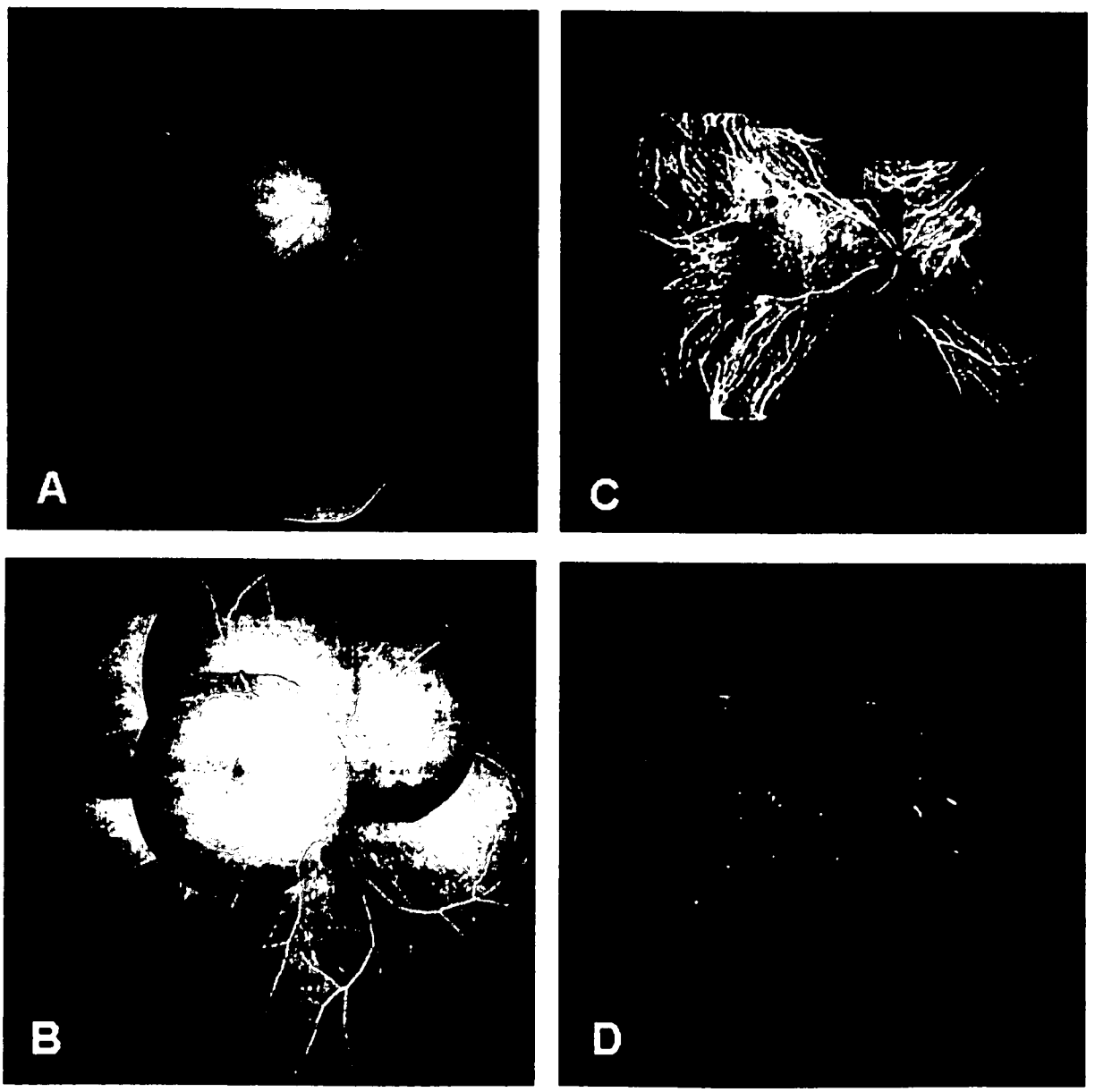

Figure 1. Case 1. The right eye appeared normal in fundus photographs (A) and fluorescein angiograms (B). Indocyanine green angiography of the right eye at 4 minutes (C) and 20 minutes (D) after dye injection. Multiple hyperfluorescent spots appeared gradually in tissue along major choroidal veins.

Case 1

A healthy 32-year-old woman noticed blurred vision and floaters in the left eye during the past year and was admitted to Kumamoto University Hospital. Abnormal conjunctival vessels, including so-called red spot or segmental and spindle-shaped dilation of conjunctival vessels,[19] were observed in both eyes, and mild vitreous opacity was identified in the left eye. A diagnosis of FAP caused by amyloidogenic transthyretin Y114C was confirmed by genetic studies.

Visual acuity (VA) in the left eye had decreased, which was correlated with the increased vitreous opacity, and vitrectomy and cataract surgeries were performed with intraocular lens (IOL) implantation when she was 34 years old. Neurological examination revealed that she had mild sensory-dominant polyneuropathy, and that year she underwent partial liver transplantation by removal of her liver and transplantation of a graft from a living related healthy donor, to prevent the production of amyloidogenic transthyretin Y114C in the liver. At the age of 35, she had vitrectomy and cataract surgery in the right eye, with IOL implantation, because of an increase in vitreous opacity. Thereafter, intraocular pressure (IOP) in the left eye gradually increased, and visual field (VF) loss worsened. Trabeculectomy in the left eye was performed when she was 39.

Ophthalmological examinations (fundus photography and FA) conducted before trabeculectomy showed normal-appearing eyes (Fig 1A, B). However, late-phase indocyanine green angiography in both eyes demonstrated multiple sites of hyperfluorescence, as identified by tissue staining along major choroidal veins (Fig 1C, D), although fundus photography and FA produced no abnormal findings at these sites, and these hyperfluorescent spots did not expand. Blood pressure (BP) was 112/52 mm Hg. The time from the onset of FAP to these examinations was 8 years. This case showed vascular lesions at an early stage. Intraocular pressure remained controlled in the postoperative period.

After liver transplantation, her polyneuropathy did not progress. Although she had no CNS disorder, magnetic resonance imaging examination after gadolinium administration indicated leptomeningeal enhancement of the spinal cord (Fig 2).

Case 2

A healthy 42-year-old woman noticed blurred vision and floaters in the right eye. At the age of 45 years, at another hospital, she underwent vitrectomy for vitreous opacity in the right eye. Glaucoma occurred when she was 46, and trabeculectomy and cataract surgery, with IOL implantation, were performed in the right eye.

At the age of 48 years, she noticed blurred vision and floaters in the left eye. Ophthalmological examination at the Kumamoto University Hospital revealed IOPs of 36 mmHg in the right eye (after maximum medical treatment) and 12 mmHg in the left eye. In addition, anterior segment examination revealed abnormal conjunctival vessels and amyloid deposition at the pupillary border, with irregularities in both eyes and rubeosis iridis in the right eye. Residual vitreous opacity in the right eye and mild vitreous opacity in the left eye were identified. That year, vitrectomy and cataract surgery in the left eye with IOL implantation were performed. Histopathological examination of vitreous materials obtained at vitrectomy revealed amyloid fibrils by means of Congo red staining, and the patient was diagnosed as having FAP caused by amyloidogenic transthyretin Y114C by means of a genetic investigation. Trabeculectomy in the right eye was not performed because she did not want to undergo the surgery.

She underwent partial liver transplantation at the age of 50 years. Nonpenetrating trabeculectomy in the left eye was performed when she was 51, but IOP increased postoperatively, and

Figure 2. Case 1. Gadolinium-enhanced T_1-weighted magnetic resonance imaging of the cervical and thoracic spinal cord. Arrows point to striking enhancement of the spinal meninges.

trabeculectomy was performed once again. Fundus photography and FA of the left eye produced no abnormal findings at that time (data not shown). Thereafter, IOP gradually increased again and was about 20 mmHg, even with maximum medical treatment.

Examination of the fundus when she was 53 years old showed pinpoint white amyloid opacities over the retinal surface, sheathing of retinal vessels, and scattered retinal hemorrhages (Fig 3A). Fluorescein angiography showed vascular closure, focal staining, and microaneurysms (Fig 3B). Panretinal photocoagulation of the vascular closure lesions was then performed. After 10 months, VA had decreased to 20/400, and IOP was 27 mmHg. Ophthalmolog-

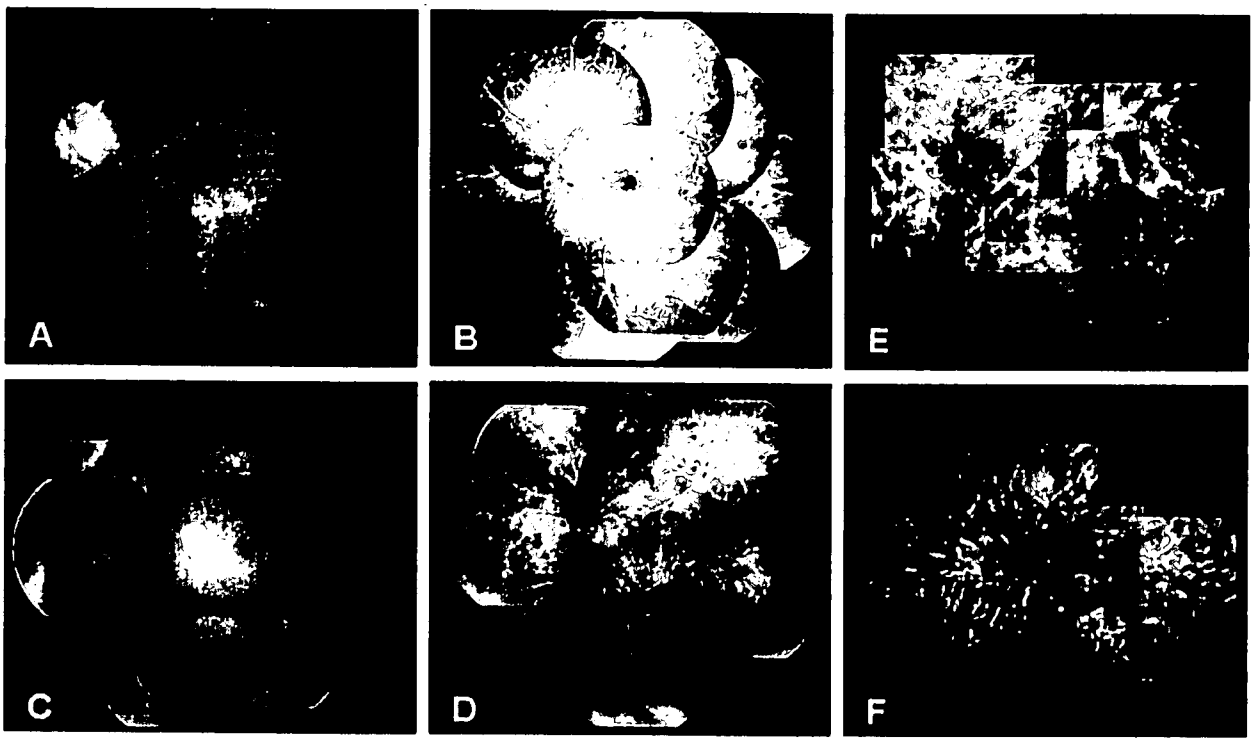

Figure 3. Case 2. A, Fundus photography of the left eye when the patient was 53 years old showed pinpoint white amyloid opacities over the retinal surface, sheathing of retinal vessels, and scattered retinal hemorrhages. B, Fluorescein angiography (FA) of the left eye at the age of 53 showed vascular closure, focal staining, and microaneurysms. C, Ten months after these examinations, examination of the fundus showed significantly greater amyloid deposition over the retinal surface, sheathing of retinal vessels, abrupt closure of vessels, and microaneurysms. D, Also 10 months later, FA showed considerably greater vascular closure, focal staining, and microaneurysms. Indocyanine green angiography of the left eye performed at the same time as C and D examinations: (E) 3 minutes and (F) 25 minutes after dye injection. Multiple sites of hyperfluorescence can be seen in tissue along retinal and choroidal vessels in the late phase.

ical reexamination (Fig 3C) revealed significantly greater amyloid deposition over the retinal surface, sheathing of retinal vessels, abrupt vessel closure, microaneurysms, and VF loss, and FA and indocyanine green angiography examinations were performed. Fluorescein angiography also demonstrated marked vascular closure, focal staining, and microaneurysms (Fig 3D). Indocyanine green angiography showed multiple sites of hyperfluorescence, with tissue staining along retinal and choroidal vessels in the late phase (Fig 3E, F). The time from onset of FAP to these examinations was 12 years. Progressive deterioration of vascular lesions was observed in this case. She has since received only topical therapy because of her poor general condition.

Although her polyneuropathy was quite mild, CNS symptoms, including fluctuating consciousness and transient right hand and leg palsy, occurred frequently, and brain magnetic resonance imaging showed ischemic changes (data not shown). Blood pressure was within the normal range.

Case 3

An apparently healthy 42-year-old woman noticed both blurred vision and floaters in both eyes. At another hospital, she underwent vitrectomy in the left eye at the age of 43 years and in the right eye 2 years later. Ophthalmological examinations at this other hospital, when the patient was 49, revealed vitreous hemorrhages related to central retinal vein occlusion and neovascular glaucoma in the left eye; vitrectomy and panretinal photocoagulation were performed. Amyloid fibrils were found by means of histopathological studies of vitreous materials obtained at vitrectomy, and she was diagnosed as having FAP caused by amyloidogenic transthyretin Y114C by means of genetic investigation. Thereafter, transpupillary photocoagulation was performed twice. At the department of cardiology of Kumamoto University Hospital, a complete atrioventricular block was discovered, and a pacemaker was implanted. The patient was admitted to the department of ophthalmology in the same year. Anterior-segment examination revealed abnormal conjunctival vessels, keratoconjunctivitis sicca, and amyloid deposition in the pupillary border in both eyes. Residual vitreous opacity in both eyes was also identified. She showed mild sensory-dominant polyneuropathy and cardiac failure.

When the patient was 52 years old, an examination of the fundus showed pinpoint white amyloid opacities over the retinal surface and the retinal vessels and mild scattered retinal hemorrhages in the peripheral fundus of the right eye. Neurological studies demonstrated CNS symptoms, including fluctuating consciousness, disorientation, and mental disturbance. Blood pressure was 92/48 mmHg. Cerebral angiography revealed a marked delay in perfusion time and enlargement of arterioles (data not shown). When the patient was 53, neovascular glaucoma occurred in the right eye; the patient's general condition then worsened, and she died of bacterial pneumonia. An autopsy was performed.

Histopathological Examinations

Autopsied organs obtained from case 3 were examined by histopathological methods. Formalin-fixed paraffin-embedded sections were stained with hematoxylin–eosin or Congo red. Speci-

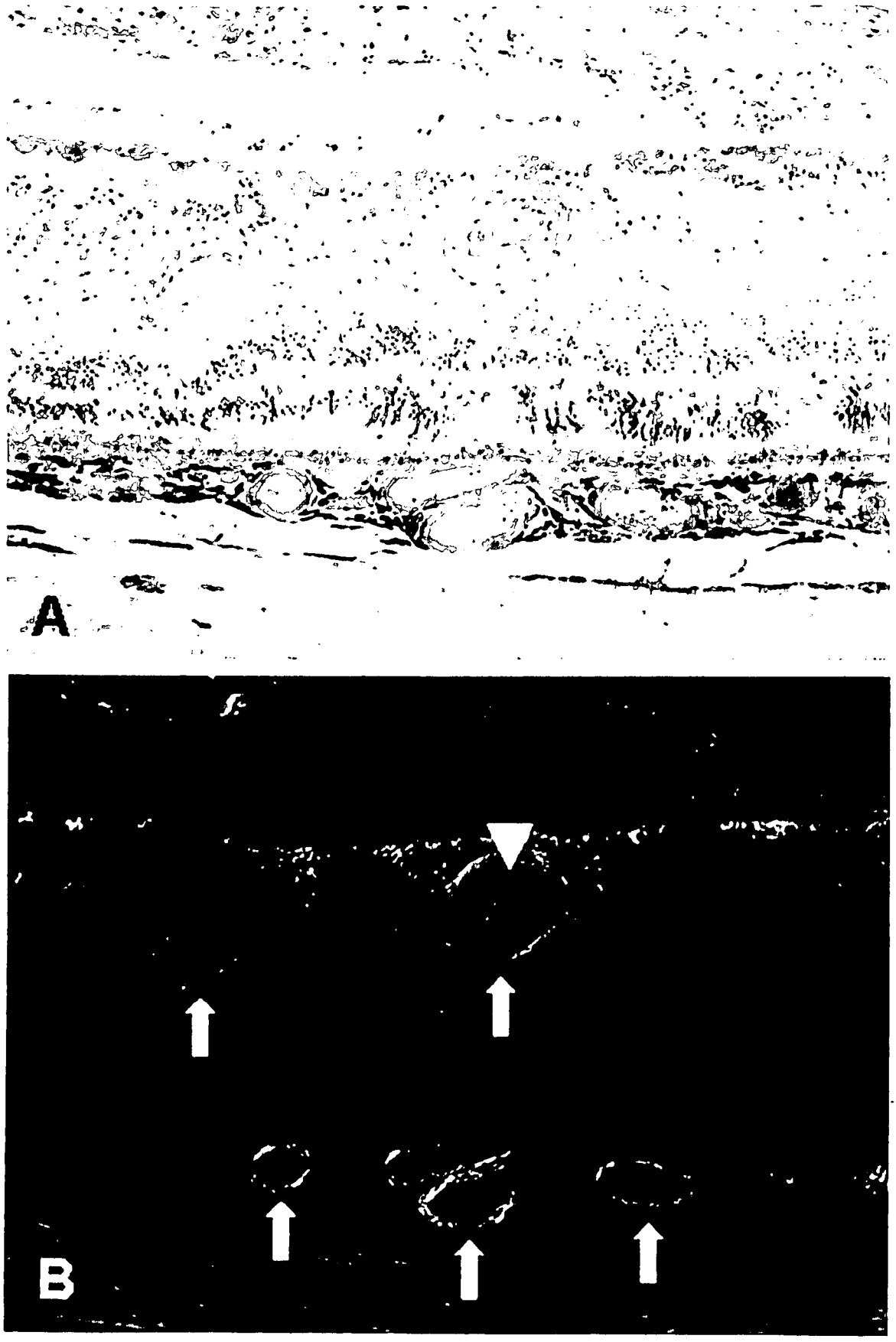

Figure 4. Case 3. Histopathological studies showed deposition of amyloid seeping through retinal vessels into vitreous and in choroidal vessels. In most vessels, amyloid deposition was found in the outer wall (arrows). Some retinal vessels had amyloid infiltration within the vessel (arrowhead). A, Stain, Congo red; original magnification, ×200. B, Stain, Congo red (viewed with polarized light); original magnification, ×200.

mens stained by Congo red were examined under polarized light for the presence of green birefringence.

Results of Histopathological Examinations

Histopathological studies of the autopsied tissues revealed deposition of amyloid seeping through retinal vessels into vitreous and in the choriocapillaris, in addition to moderate to marked amyloid deposition in peripheral nerves, the heart, kidney, gastrointestinal tract, lung, leptomeninges, and edges of the spinal cord. Amyloid deposition in the perivascular wall areas was common in these tissues, but considerable amyloid deposition was observed within the retinal vessels (Fig 4).

Discussion

In this report, we present clinicopathological findings for patients with FAP caused by amyloidogenic transthyretin Y114C and summarize unique retinal and choroidal vascular lesions.

Fluorescein angiography confirmed the presence of the retinal vascular manifestations of sheathing or closure of retinal vessels and scattered retinal hemorrhages in the peripheral region of the fundus, as evidenced by focal staining and microaneurysms. Maeda et al[19] have postulated that in CAA-related intracerebral hemorrhage caused by deposition of Aβ amyloid, vascular amyloid deposition leads to degeneration and loss of smooth muscle cells of the media, followed by microaneurysmal dilation, fibrinoid necrosis, and then vessel wall rupture. The mechanism of intraretinal hemorrhage in FAP caused by amyloidogenic transthyretin Y114C may be fundamentally similar to that just noted, because patients had normal or low BP and no trigger factors other than amyloid deposits. However, changes in ocular vessels have not been studied, and such changes may also occur in other types of CAA.

We previously reported that the prevalence of vitreous opacities in patients with FAP caused by amyloidogenic transthyretin Y114C was significantly higher and the age at onset of these opacities was significantly lower than those in patients with FAP caused by amyloidogenic transthyretin V30M.[13] In addition, previous clinical and histopathological reports included few cases of retinal or choroidal vascular lesions in FAP caused by amyloidogenic transthyretin V30M.[3,15,20–24] In most patients with FAP caused by amyloidogenic transthyretin V30M, retinal vessels appeared normal, and perivascular infiltrates, white sheathing of retinal vessels, and retinal hemorrhages showing leakage via FA were rarely observed. In contrast, in our clinicopathological examinations reported here, patients with FAP caused by amyloidogenic transthyretin Y114C showed severe and progressive changes in retinal or choroidal vascular lesions. Various factors, such as environmental ones or penetrance in addition to the substitution of amino acids at different positions, may cause these different phenotypes.

Important tissues for synthesis and secretion of pathogenic transthyretin include, in addition to the liver,[25] the retinal pigment epithelium (RPE)[26,27] and choroid plexus of the brain.[28–30] Liver transplantation is widely accepted as an effective means of halting amyloid deposition in systemic tissues,[31,32] because transthyretin that circulates in serum is synthesized predominantly by the liver. However, even after liver transplantation the RPE still synthesizes variant transthyretin, and vitreous amyloid deposition and glaucoma may result.[33–36] In case 2, we newly found progressive changes in retinal vascular lesions due to amyloid deposition even after liver transplantation. Variant transthyretin synthesized by RPE, which is secreted into the sensory retina, may cause vascular amyloid deposition, resulting in a steno-occlusive vascular disorder.

Finally, in case 1 (with an earlier stage of disease than the other 2 cases) we found amyloid deposition in choroidal vessels, whereas retinal vessels appeared almost normal. Thus, indocyanine green angiography examination may help detect early changes in ocular vascular lesions in patients with FAP.

Familial amyloidotic polyneuropathy caused by amyloidogenic transthyretin Y114C induces ocular amyloid angiopathy as well as CAA. Severe and progressive retinal and choroidal vascular lesions, which caused visual disturbances, were seen in these patients. For improved understanding of this disorder, similar studies of patients with other types of FAP should be performed.

References

1. Vinters HV, Gilbert JJ. Cerebral amyloid angiopathy: incidence and complications in the aging brain. II. The distribution of amyloid vascular changes. Stroke 1983;14:924–8.
2. Yong WH, Robert ME, Secor DL, et al. Cerebral hemorrhage with biopsy-proved amyloid angiopathy. Arch Neurol 1992; 49:51–8.
3. Uitti RJ, Donat JR, Rozdilsky B, et al. Familial oculoleptomeningeal amyloidosis. Report of a new family with unusual features. Arch Neurol 1988;45:1118–22.
4. Kametani F, Ikeda S, Yanagisawa N, et al. Characterization of a transthyretin-related amyloid fibril protein from cerebral amyloid angiopathy in type I familial amyloid polyneuropathy. J Neurol Sci 1992;108:178–83.
5. Garzuly F, Vidal R, Wisniewski T, et al. Familial meningocerebrovascular amyloidosis, Hungarian type, with mutant transthyretin (TTR Asp18Gly). Neurology 1996;47:1562–7.
6. Vidal R, Garzuly F, Budka H, et al. Meningocerebrovascular amyloidosis associated with a novel transthyretin mis-sense mutation at codon 18 (TTRD 18G). Am J Pathol 1996;148: 361–6.
7. Sakashita N, Ando Y, Jinnouchi K, et al. Familial amyloidotic polyneuropathy (ATTR Val30Met) with widespread cerebral amyloid angiopathy and lethal cerebral hemorrhage. Pathol Int 2001;51:476–80.
8. Araki S. Type I familial amyloidotic polyneuropathy [in Japanese]. No To Hattatsu 1984;16:92–100.
9. Ando Y, Araki S, Shimoda O, Kano T. Role of autonomic nerve functions in patients with familial amyloidotic polyneuropathy as analyzed by laser Doppler flowmetry, capsule hydrograph, and cardiographic R-R interval. Muscle Nerve 1992;15:507–12.
10. Connors LH, Lim A, Prokaeva T, et al. Tabulation of human transthyretin (TTR) variants, 2003. Amyloid 2003;10:160–84.
11. Sandgren O. Ocular amyloidosis, with special reference to the hereditary forms with vitreous involvement. Surv Ophthalmol 1995;40:173–96.

12. Ando E, Ando Y, Okamura R, et al. Ocular manifestations of familial amyloidotic polyneuropathy type I: long-term follow up. Br J Ophthalmol 1997;81:295–8.
13. Koga T, Ando E, Hirata A, et al. Vitreous opacities and outcome of vitreous surgery in patients with familial amyloidotic polyneuropathy. Am J Ophthalmol 2003;135:188–93.
14. Kimura A, Ando E, Fukushima M, et al. Secondary glaucoma in patients with familial amyloidotic polyneuropathy. Arch Ophthalmol 2003;121:351–6.
15. Savage DJ, Mango CA, Streeten BW. Amyloidosis of the vitreous. Fluorescein angiographic findings and association with neovascularization. Arch Ophthalmol 1982;100:1776–9.
16. Futa R, Inada K, Nakashima H, et al. Familial amyloidotic polyneuropathy: ocular manifestations with clinicopathological observation. Jpn J Ophthalmol 1984;28:289–98.
17. Ueno S, Fujimura H, Yorifuji S, et al. Familial amyloid polyneuropathy associated with the transthyretin Cys114 gene in a Japanese kindred. Brain 1992;115:1275–89.
18. Haagsma EB, Post JG, De Jager AE, et al. Familial amyloidotic polyneuropathy with severe renal involvement in association with transthyretin Gly47Glu in Dutch, British and American-Finnish families. Amyloid 2004;11:44–9.
19. Maeda A, Yamada M, Itoh Y, et al. Computer-assisted three-dimensional image analysis of cerebral amyloid angiopathy. Stroke 1993;24:1857–64.
20. Schwartz MF, Green WR, Michels RG, et al. An unusual case of ocular involvement in primary systemic nonfamilial amyloidosis. Ophthalmology 1982;89:394–401.
21. Tsukahara S, Matsuo T. Fluorographical findings in familial primary amyloidosis. Ophthalmologica 1978;176:301–7.
22. Inomata H, Okayama M, Oshima K. Familial primary amyloidosis, light and electron microscopic histopathology of the eye. Jpn J Ophthalmol 1976;20:51–62.
23. Kojima A, Ohno-Matsui K, Mitsuhashi T, et al. Choroidal vascular lesions identified by ICG angiography in a case of familial amyloidotic polyneuropathy. Jpn J Ophthalmol 2003; 47:97–101.
24. Dunlop AA, Graham SL. Familial amyloidotic polyneuropathy presenting with rubeotic glaucoma. Clin Experiment Ophthalmol 2002;30:300–2.
25. Felding P, Fex G. Cellular origin of prealbumin in the rat. Biochim Biophys Acta 1982;716:446–9.
26. Martone RL, Schon EA, Goodman DS, et al. Retinol-binding protein is synthesized in the mammalian eye. Biochem Biophys Res Commun 1988;157:1078–84.
27. Cavallaro T, Martone RL, Dwork AJ, et al. The retinal pigment epithelium is the unique site of transthyretin synthesis in the rat eye. Invest Ophthalmol Vis Sci 1990;31:497–501.
28. Soprano DR, Herbert J, Soprano KJ, et al. Demonstration of transthyretin mRNA in the brain and other extrahepatic tissues in the rat. J Biol Chem 1985;260:11793–8.
29. Herbert J, Wilcox JN, Pham KT, et al. Transthyretin: a choroid plexus-specific transport protein in human brain. The 1986 S. Weir Mitchell award. Neurology 1986;36:900–11.
30. Dickson PW, Howlett GJ, Schreiber G. Rat transthyretin (prealbumin). Molecular cloning, nucleotide sequence, and gene expression in liver and brain. J Biol Chem 1985;260:8214–9.
31. Holmgren G, Steen L, Ekstedt J, et al. Biochemical effect of liver transplantation in two Swedish patients with familial amyloidotic polyneuropathy (FAP-met30). Clin Genet 1991; 40:242–6.
32. Ando Y, Tanaka Y, Nakazato M, et al. Change in variant transthyretin levels in patients with familial amyloidotic polyneuropathy type I following liver transplantation. Biochem Biophys Res Commun 1995;211:354–8.
33. Ando Y, Ando E, Tanaka Y, et al. De novo amyloid synthesis in ocular tissue in familial amyloidotic polyneuropathy after liver transplantation. Transplantation 1996;62:1037–8.
34. Ando E, Ando Y, Haraoka K. Ocular amyloid involvement after liver transplantation for polyneuropathy [letter]. Ann Intern Med 2001;135:931–2.
35. Munar-Ques M, Salva-Ladaria L, Mulet-Perera P, et al. Vitreous amyloidosis after liver transplantation in patients with familial amyloid polyneuropathy: ocular synthesis of mutant transthyretin. Amyloid 2000;7:266–9.
36. Haraoka K, Ando Y, Ando E, et al. Presence of variant transthyretin in aqueous humor of a patient with familial amyloidotic polyneuropathy after liver transplantation. Amyloid 2002;9:247–51.

Table 1. Clinical Characteristics of Patients with Familial Amyloidotic Polyneuropathy (FAP) Amyloidogenic Transthyretin Y114C

Measure	Case 1, Female		Case 2, Female		Case 3, Female	
Age at onset of FAP (yrs)	31		42		42	
Eye affected	R	L	R	L	R	L
Visual acuity at first visit	20/20	20/40	20/200	20/30	20/20	HM
Age at onset of vitreous opacity (yrs)	33	31	42	47	42	42
Age at time of vitrectomy (yrs)	35	34	45	48	45	43, 49
Age at onset of glaucoma (yrs)	38	37	46	49	53	49
Age at time of glaucoma surgery (yrs)	NA	39	46	51	NA	49
Age at time of FA examination (yrs)	39	39	ND	51, 53, 54	ND	ND
Age at time of IA examination (yrs)	39	39	ND	54	ND	ND
Age at time of liver transplantation (yrs)	34		50		NA	
CNS symptoms						
Drowsiness	+		−		−	
Mental disorder	−		−		−	
Dementia	−		−		+	
LOC episodes	+		−		−	
TIA-like episodes	+		+		−	
Pyramidal signs	+		+		−	
Extrapyramidal signs	−		+		−	
Cerebral hemorrhage	−		−		+	
Brain infarction	−		−		−	
Meningeal enhancement on spinal cord MRI	+		+		ND	

CNS = central nervous system; FA = fluorescein angiography; HM = hand movements; IA = indocyanine green angiography; L = left; LOC = loss of consciousness; MRI = magnetic resonance imaging; NA = not applicable; ND = examination not done; R = right; TIA = transient ischemic attack. +, symptom detectable; −, symptom not detectable.

The Effect of Subtenon Triamcinolone Acetonide Injection for Diabetic Macular Edema on Retinal and Choroidal Circulation

Yuki Mawatari, MD, Tomoyo Koga, MD, Junko Inumaru, MD, Akira Hirata, MD, PhD, Mikiko Fukushima, MD, PhD, and Hidenobu Tanihara, MD, PhD

PURPOSE: To evaluate changes in retinal and choroidal circulation after subtenon triamcinolone acetonide (TA) injection for diabetic macular edema.

DESIGN: Prospective interventional case series.

METHODS: Thirteen eyes of 13 patients with diabetic macular edema were studied. Fluorescein and indocyanine green angiograms were performed at three periods: before the injection and 1 week and 6 months after subtenon injection of TA (40 mg). Retinal arteriovenous passage time (as an indicator of retinal circulation) and choroidal τ (as an indicator of early filling velocity of choroid) were obtained with image analysis software.

RESULTS: Choroidal τ values before and 1 week after subtenon TA injection were, respectively, 3.2 ± 0.4 and 4.0 ± 0.7 seconds, which showed a significant delay ($P = .01$, Wilcoxon signed-rank test). The delayed choroidal τ values returned to pretreatment level at 6 months after TA injection. In contrast, the arteriovenous passage time remained unchanged.

CONCLUSION: Subtenon TA injection transiently influences choroidal blood flow. (Am J Ophthalmol 2005; 140:948–949. © 2005 by Elsevier Inc. All rights reserved.)

RECENT CLINICAL STUDIES HAVE SUGGESTED THAT INtravitreal or subtenon injection of triamcinolone acetonide (TA) was effective for the treatment of diabetic macular edema (DME).[1,2] The mechanisms underlying the effects of corticosteroid on DME have not been clarified; however, corticosteroids exhibit a vasoconstrictive effect, and the topical application of corticosteroids induces blanching of skin as a result of changes to the underlying microcirculation of the skin.[3] These findings imply that topical corticosteroid treatment may influence ocular circulation. The quantification of ocular circulation is made possible through the use of videoangiograms and image analysis techniques.[4] In our present study, we measured retinal and choroidal circulation quantitatively using these methods and report that choroidal circulation is altered transiently after subtenon TA injection.

After informed consent had been obtained, 13 eyes of 13 patients (10 male and three female patients; aged, 61.6 ± 12.9 years) underwent posterior subtenon TA injection (40 mg) and were followed for >6 months. Fluorescein and indocyanine green angiograms with a scanning laser ophthalmoscope (Rodenstock Instrument, Inc, Munich, Germany) were performed before and 1 week and 6 months after the initiation of subtenon TA injection. Ocular perfusion pressure (calculated with blood pressure and intraocular pressure) was also measured. Fluorescein and indocyanine green angiograms were captured with image analysis software (DIPP-MOTION 2 diopters; Ditect, Tokyo, Japan), and the dye intensity curve was obtained with this software. Retinal arteriovenous passage time was measured as an indicator of retinal circulation and represents the time lapse between 50% of the peak intensity of a paired artery and vein.[4] Choroidal τ (the time constant) was measured as an indicator of early filling velocity of choroid and represents the time lapse between the initiation and 0.63% of the maximal intensity of choroidal dye background.[4] Consequently, if early filling velocity of choroid decrease, choroidal τ will be delayed. The Wilcoxon signed-rank test was performed for statistical analysis. A probability value $<.05$ was considered statistically significant.

No significant changes of ocular perfusion pressure after subtenon TA injection were observed. However, choroidal τ values before and 1 week after subtenon TA injection were 3.2 + 0.4 and 4.0 ± 0.7 seconds, respectively, which shows a significant delay ($P = .01$, Wilcoxon signed-rank test; Table). In addition, subtenon TA mass was not observed in the B-mode ultrasonography. The delayed choroidal τ values returned to pretreatment level at 6 months after subtenon TA injection. In contrast, the retinal arteriovenous passage time remained unchanged after subtenon TA injection. The central retinal thickness decreased significantly after subtenon TA injection that was measured by optical coherence tomography (Humphrey model 2000; Humphrey Instruments, San Leandro, California, USA). No eye showed decreased visual acuity after subtenon TA injection.

Previous studies demonstrated significant relationships between choroidal blood flow and ocular perfusion pressure.[5] Although the ocular perfusion pressure in DME patients did not change after subtenon TA injection, the early filling velocity of choroid decreased significantly at 1 week after subtenon TA injection. Considering that no mass effect after subtenon TA injection was observed, subtenon TA injection affects choroidal vascular resistance and changes choroidal circulation. We speculate that a corticosteroid-induced vasoconstrictive effect plays a role in the alterations of choroidal circulation.[3,6] In

Accepted for publication Jun 1, 2005.

From the Department of Ophthalmology and Visual Science, Graduate School of Medical Sciences, Kumamoto University, Kumamoto, Japan.

Supported in part by a Grant-in-Aid for Scientific Research from the Ministry of Education, Science, Sport and Culture, and the Ministry of Health and Welfare, Japan.

Inquiries to Hidenobu Tanihara, MD, PhD, Department of Ophthalmology and Visual Science, Graduate School of Medical Sciences, Kumamoto University, 1, Honjo, Kumamoto, 860-8556, Japan; fax: +81-96-373-5249; e-mail: tanihara@pearl.ocn.ne.jp

TABLE. Changes of Intraocular Pressure, Ocular Profusion Pressure, Arteriovenous Passage Time, Choroidal τ, and Retinal Thickness Before and After Sub-Tenon TA injection

Variable	Before treatment at baseline (mean ± SD)	1 Wk after TA injection		6 Mo after TA injection	
		Mean ± SD	*P* value	Mean ± SD	*P* value
Intraocular pressure (mm Hg)	15.2 ± 3.5	16.1 ± 3.4	.02	16.0 ± 4.6	.21
Ocular profusion pressure (mm Hg)	83.0 ± 11.7	82.0 ± 12.1	.12	82.2 ± 10.8	.44
AVP time (sec)	1.7 ± 0.6	1.8 ± 0.5	.55	1.6 ± 0.4	.57
Choroidal τ (sec)	3.2 ± 0.4	4.0 ± 0.7	.01	3.3 ± 0.6	.37
Retinal thickness (μm)	583 ± 127	425 ± 132	.002	292 ± 135	<.001

contrast, the retinal circulation in patients with DME did not change after subtenon TA injection. The pharmacodynamics of TA after subtenon injection have not been clarified, but the episcleral implant of corticosteroid shows that corticosteroid penetrates through the sclera and disperses into the retinochoroid.[7] We therefore believe that the subtenon TA injection can affect the choroidal tissue much more than its effects on the retina. In addition, our results showed that the inhibitory effects on choroidal circulation were only transient and did not result in visual dysfunction. However, attention should be paid to the extensive or repeated use of subtenon TA injection in patients with DME.

In conclusion, subtenon TA injection transiently influences choroidal blood flow but does not result in a disturbance of visual function.

REFERENCES

1. Jonas JB, Sofker A. Intraocular injection of crystalline cortisone as adjunctive treatment of diabetic macular edema. Am J Ophthalmol 2001;132:425–427.
2. Bakri SJ, Kaiser PK. Posterior subtenon triamcinolone acetonide for refractory diabetic macular edema. Am J Ophthalmol 2005;139:290–294.
3. Sommer A, Lucassen GW, Houben AJ, Neumann MH. Vasoconstrictive effect of topical applied corticosteroids measured by laser Doppler imaging and reflectance spectroscopy. Microvasc Res 2003;65:152–159.
4. Duijm HF, van den Berg TJ, Greve EL. A comparison of retinal and choroidal hemodynamics in patients with primary open-angle glaucoma and normal-pressure glaucoma. Am J Ophthalmol 1997;123:644–656.
5. Riva CE, Titze P, Hero M, Movaffaghy A, Petrig BL. Choroidal blood flow during isometric exercises. Invest Ophthalmol Vis Sci 1997;38:2338–2343.
6. Drescher W, Weigert KP, Bunger MH, Ingerslev J, Bunger C, Hansen ES. Femoral head blood flow reduction and hypercoagulability under 24 h megadose steroid treatment in pigs. J Orthop Res 2004;22:501–508.
7. Kato A, Kimura H, Okabe K, Okabe J, Kunou N, Ogura Y. Feasibility of drug delivery to the posterior pole of the rabbit eye with an episcleral implant. Invest Ophthalmol Vis Sci 2004;45:238–244.

Vogt-Koyanagi-Harada Disease in Patients With Chronic Hepatitis C

Valérie Touitou, MD, Bahram Bodaghi, MD, PhD, Nathalie Cassoux, MD, Thi Ha Chau Tran, MD, Narsing A. Rao, MD, Patrice Cacoub, MD, and Phuc LeHoang, MD, PhD

PURPOSE: To report the cases of four patients with hepatitis C virus infection who experienced clinical features that are virtually identical to Vogt-Koyanagi-Harada disease (VKH).

DESIGN: Retrospective observational case series.

METHODS: Medical records of patients who were referred between January and December 2003 were reviewed for diagnosis and management of VKH and who also had chronic hepatitis C virus (HCV) infection.

RESULTS: Four white patients had the clinical features of VKH. Three of the patients experienced intraocular inflammation while they were being treated for HCV infection with pegylated interferon alpha 2b and ribavirin. The intraocular inflammation responded to systemic corticosteroid treatment and to discontinuation of antiviral agents.

CONCLUSION: Although the number of patients who were studied is limited, there appears to be an association between HCV infection that was treated with pegylated interferon alpha 2b and the development of VKH-like disease. Further studies are required to confirm such an association. (Am J Ophthalmol 2005;140:949–952.

Accepted for publication Jun 11, 2005.

From the Departments of Ophthalmology (V.T., B.B., N.C., C.H.C.T., P.L.) and Internal Medicine (P.C.), Pitié-Salpêtrière Hospital, Paris, France; and Doheny Eye Institute, Los Angeles, California USA (R.A.R.).

Inquiries to P. LeHoang, Service d'Ophtalmologie, Pitié-Salpêtrière Hospital, 43 bd de l'Hôpital, 75013 Paris, France; fax: 33-1-42163218; e-mail: bahram.bodaghi@psl.ap-hop-paris.fr.

Intravitreal Plasmin Injection Activates Endogenous Matrix Metalloproteinase-2 in Rabbit and Human Vitreous

AKIOMI TAKANO, MD, AKIRA HIRATA, MD, PHD, YASUYA INOMATA, MD, TAKAHIRO KAWAJI, MD, KUNIKO NAKAGAWA, SHIROU NAGATA, AND HIDENOBU TANIHARA, MD, PHD

• PURPOSE: To investigate the effect of exogenous plasmin administration on the activity of endogenous matrix metalloproteinase-2 (MMP-2) in rabbit and human vitreous.

• DESIGN: Experimental animal study and interventional case series.

• METHODS: Human plasmin was injected into rabbit eyes. The active/pro-MMP-2 ratio in vitreous samples was calculated using the gelatin zymography. Scanning electron microscopy (SEM) was performed to observe the retinal surface. To evaluate the time course of MMP-2 activity, vitreous samples were collected after the injection of 0.5 IU of plasmin, and the active/pro-MMP-2 ratio was calculated in the same manner. Immunohistochemical analysis was performed to confirm the presence of MT1-MMP in the rabbit eye. Human vitreous samples obtained from vitreous surgeries were also used for similar studies.

• RESULTS: The active/pro-MMP-2 ratios in the vitreous after the injection of 0.25 IU or 0.5 IU of plasmin were significantly higher than that of the control ($P < .05$). SEM demonstrated that plasmin-treated eyes showed a smooth retinal surface that was dose-dependent. Time course evaluation of the active/pro-MMP-2 ratio in the vitreous after the administration of 0.5 IU of plasmin found a significant difference between the 5 and 15 minutes data points compared with that seen for the control. Immunohistochemical study revealed the presence of MT1-MMP in the inner retina. In human samples, the active/pro-MMP-2 ratio after the plasmin injection was significantly higher than the ratio observed before injection.

• CONCLUSIONS: Our results suggested that activation of endogenous MMP-2 by exogenous plasmin is associated with the induction of posterior vitreous detachment. (Am J Ophthalmol 2005;140:654–660. © 2005 by Elsevier Inc. All rights reserved.)

PARS PLANA VITRECTOMY WITH ARTIFICIAL POSTERIOR vitreous detachment (PVD) contributes to the successful treatment of a number of vitreoretinal diseases. However, in some cases it is difficult to induce complete PVD. Moreover, residual vitreous often causes severe complications, such as proliferative vitreoretinopathy.

Recent reports indicate that plasmin is a useful adjunctive that can be used to liquefy the vitreous gel and induce PVD. This procedure leads to the reduction of the mechanical suction levels and decreases complications.[1–9] However, little information is available on the mechanism of induction of PVD by plasmin.

Matrix metalloproteinases (MMPs) are a family of proteolytic enzymes that function to maintain and/or remodel tissue architecture.[10] They are mostly secreted as inactive proenzymes and are cleaved extracellularly to become the functionally active form. To date, MMPs have been found in virtually every tissue of the eye both in healthy subjects and those with diseases.[11] MMP-2 is a member of the matrixin enzyme family and has been identified previously in the human vitreous.[11–16] Because of its ability to degrade type IV collagen, MMP-2 is believed to be necessary for basement membrane degradation, and its activity to degrade various collagens has been considered to be a potential mechanism for the vitreous liquefaction that is seen in aging and various pathologic states.[13,14,17]

Pro-MMP-2 activation is thought to be a two-step process. In the first step, membrane-type 1 matrix metal-

Accepted for publication Apr 5, 2005.

From the Department of Ophthalmology and Visual Science, Kumamoto University Graduate School of Medical Sciences, Kumamoto, Japan (A.T., A.H., Y.I., T.K., H.T.); and the Department of Clinical Laboratory, Kumamoto University Hospital, Kumamoto, Japan (K.N., S.N.).

Supported in part by a Grant-in-Aid for Scientific Research from the Ministry of Education, Science, Sports and Culture, Japan from the Ministry of Health and Welfare, Japan.

Inquiries to Hidenobu Tanihara, MD, PHD, Department of Ophthalmology and Visual Science, Kumamoto University Graduate School of Medical Sciences, 1-1-1 Honjo, Kumamoto 860-8556, Japan; fax: 011-81-96-373-5249; e-mail: tanihara@pearl.ocn.ne.jp

0002-9394/05/$30.00
doi:10.1016/j.ajo.2005.04.017

loproteinase (MT1-MMP) generates the intermediate form of MMP-2, which is followed by an intermolecular autocatalytic reaction in the second step that results in the formation of active MMP-2.[18] MT1-MMP attaches to the cell surface through a transmembrane domain and activates the pro-MMP-2 at the cell surface.[18] However, distribution of the MT1-MMP in the retina has not been fully described. Previous studies suggest that plasmin cooperates with MT1-MMP in the activation of pro-MMP-2.[19-21] Therefore, we hypothesized that exogenous plasmin induces PVD by increasing the ratio of active MMP-2 in the vitreous.

The present study addressed four issues. First, we measured the active MMP-2 level after the injection of various doses of plasmin. Second, we analyzed the time course of MMP-2 activity after plasmin administration. Third, we tried to identify the location of MT1-MMP in the retina. Fourth, we investigated the MMP-2 activity before and after injections of plasmin in human vitreous. MMP-2 was determined using gelatin zymography, and the presence of MT1-MMP in the retina was determined by immunohistochemistry. After injection of various doses of plasmin, the retinal surface was observed by scanning electron microscopy (SEM).

MATERIALS AND METHODS

• ANIMALS: Japanese adult albino rabbits (Kyudo, Kumamoto, Japan), which were 12 weeks of age and weighed 2.0 kg to 2.5 kg, were used in this experimental animal study and interventional case series. The animals were treated in accordance with the ARVO Statement for the Use of Animals in Ophthalmic and Vision Research and the guidelines of the Committee on Animal Research of Kumamoto University. The rabbits were kept anesthetized throughout the entire period of the experiment.

• PLASMIN PREPARATION: Human plasminogen was purified as described previously.[4-6] Briefly, human blood was obtained from healthy subjects and drawn from the antecubital fossa. Samples were centrifuged at 2300 rpm for 15 minutes at 4 C, resulting in fresh human plasma. The plasminogen was purified from the human plasma by affinity chromatography on a lysine-sepharose column. The plasminogen was eluted with 15 mmol/l ϵ-aminocaproic acid. The ϵ-aminocaproic acid was removed by overnight dialysis, and the plasminogen concentrated to a final volume of 0.5 ml. An aliquot was tested for sterility. Just before the injection into the vitreous, the plasminogen was converted to plasmin by adding 2500 IU of urokinase for 15 minutes under room temperature followed by sterilization by passage through a 0.22 μm filter. The plasmin activity was tested immediately by measuring the change in absorbency at 405 nm after cleavage of the D-Val-Leu-Lys p-nitroanilide dihydrochloride substrate (Sigma-Aldrich; St. Louis, Missouri, USA) spectrophotometrically and then stored at 4 C until use. The plasmin solution was diluted with sterile balanced salt solution (BSS Plus; Alcon Surgical, Tokyo, Japan) to final concentrations of 0.05, 0.25, and 0.5 IU/50 μl.

• PLASMIN ADMINISTRATION AND VITRECTOMY: The rabbits were anesthetized with pentobarbital (20 mg/kg intravenously, Nembutal; Dainippon Pharmaceuticals, Osaka, Japan) and ketamine hydrochloride (20 mg/kg intramuscularly, Ketaral 50; Sankyo Pharmaceuticals, Tokyo, Japan). The pupils were dilated with a mixture of tropicamide 0.5% and phenylephrine hydrochloride 0.5%. Pars plana injection of the plasmin solution was performed 2 mm from the limbus with a 1-ml syringe (Terumo, Tokyo, Japan). For the dose study, 12 rabbit eyes were randomly divided into three groups. Four eyes in each of three different groups received 50 μl injections of 0.05, 0.25, and 0.5 IU of human plasmin, respectively. Using the same method, four other rabbit eyes that served as controls were given pars plana injections of 50 μl BSS into the vitreous cavity.

Fifteen minutes after the injection of plasmin or BSS, undiluted vitreous samples of approximately 1.0 ml were collected. Briefly, a scleral incision was made 2 mm from the limbus with a 20-degree knife (MVR20; Mani, Tochigi, Japan). Without the use of any infusion, a vitreous cutter (Alcon, Tokyo, Japan) was inserted gently through the scleral incision into the midvitreous cavity. Undiluted vitreous sample was collected through active aspiration with cutting and scleral indentation.

To investigate the time course of the MMP-2 activity, twenty rabbit eyes underwent pars plana injection of 0.5 IU human plasmin into the vitreous cavity. Pars plana vitrectomy was performed as described above. Four eyes in each of the groups had vitrectomies at 5, 15, 30, 120, and 360 minutes after the plasmin injections, respectively. The samples were immediately stored in Eppendorf tubes and centrifuged at 10000 g for 20 minutes at 4 C, and the supernatant was transferred to a clean tube and stored at −80 C until use.

• GELATIN ZYMOGRAPHY: To detect the activation ratio of MMP-2, samples were analyzed by gelatin zymography using a commercially available kit (Gelatinzymo Electrophoresis Kit; Yagai Research Center, Yamagata, Japan). This assay was performed according to the supplied protocol. Briefly, 10 μl of each sample was mixed with the same amount of buffer (50 mmol/l Tris-HCl buffer, pH 6.8, which contained SDS, glycerol, and bromphenol blue), and incubated at room temperature for 15 minutes. The samples were electrophoresed at 10 mA for 20 minutes and then at 20 mA for 120 minutes until the dye front reached the bottom of the gel (Precast 7.5% polyacrylamide minigels containing sodium dodecyl sulfate 0.3% and 1 mg/ml of gelatin). Supplied markers containing active MMP-2, pro-MMP-2, and pro-MMP-9 were also loaded onto the gel as references. After electrophoresis, the gels were agitated

in Triton X-100 buffer for 30 minutes to remove the SDS and then mixed with 50 mmol/l Tris-HCl buffer, pH 7.5, containing NaCl and shaken for 30 minutes to restore the enzymatic activity. Samples were then incubated in 50 mmol/l Tris-HCl buffer, pH 7.5, containing 200 mmol/l NaCl and 5 mmol/l CaCl2 at 37 C for 26 hours to allow proteolysis of the gelatin. Subsequently, the gels were stained for 30 minutes with Coomassie Blue G25. Finally, the gels were destained in methanol 30% and acetic acid 5% at room temperature for 3 hours. The negatively stained bands were detected by means of comparisons to the supplied markers.

An image scanner was used to scan the gels and the areas of the bands corresponding to MMP-2 activity were analyzed by NIH Image 1.63 software (developed at the US National Institutes of Health; available at http://rsb.info.nih.gov/nih-image/). Determination of the band intensity was performed as described in the tutorial for the NIH Image software. Individual values were calibrated by referring to the clear band area of the MMP-2 standard that was injected with the samples in the each of the gels. The activation ratio of MMP-2 (active/pro-MMP-2 ratio) was calculated by dividing the intensity of the band for the active form by the intensity of the band for latent form of MMP-2.

• SCANNING ELECTRON MICROSCOPY: Twelve eyes were studied using SEM. Thirty minutes after the injection of BSS or the different doses of plasmin (0.05, 0.25, or 0.5 IU), the animals were killed with an overdose of an intravenous injection of pentobarbital. The eyes were immediately enucleated and immersed in a fixative that consisted of a glutaraldehyde 2.5% and paraformaldehyde 2% mixture in 0.1 mol/l phosphate buffer at room temperature for 2 hours. The eyes were cut circumferentially at the limbus to make posterior cups and then immersed in the fixative for an additional hour. The specimens were immersed in tannic acid 2% (Wako, Osaka, Japan) overnight at room temperature to increase tissue reactivity with the osmium tetroxide, rinsed with distilled water for 2 hours, and then fixed with osmium tetroxide 1% for 2 hours at 4 C. The specimens were dehydrated in a graded ethanol series, infiltrated in 100% t-butanol, frozen, freeze-dried by evaporation in a vacuum, mounted on aluminum stubs, and then gold coated. They were observed at an accelerating voltage of 15 kV to 20 kV with a scanning electron microscope (JSM 6400FK; Jeol, Tokyo, Japan).

• IMMUNOHISTOCHEMISTRY FOR MT1-MMP: To detect the localization of MT1-MMP, immunohistochemical staining was performed. After the animals were killed with an overdose of an intravenous injection of pentobarbital, the eyes were enucleated. The eyes were fixed in paraformaldehyde 4% in phosphate buffered saline at 4 C overnight, and embedded in paraffin. The 5 μm thick serial sections were incubated with hydrogen peroxide for 5 minutes, and were reacted overnight at 4 C with mouse

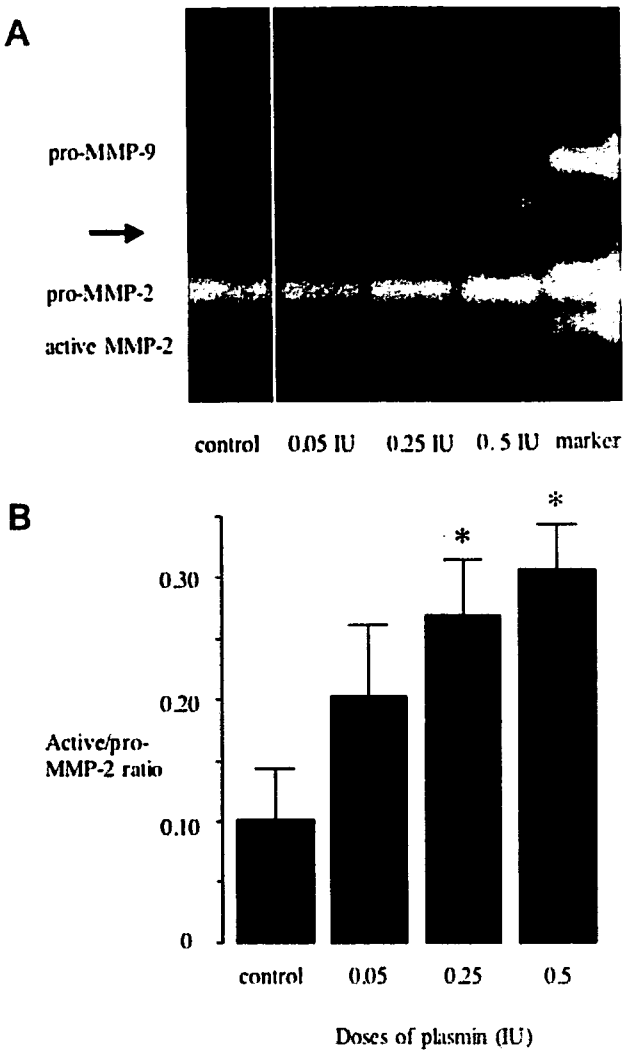

FIGURE 1. (A) Gelatin zymography of the vitreous samples from rabbits after injections of 0.05, 0.25, and 0.5 IU of plasmin. The activity is visualized as the clear band, the positive markers indicate pro-MMP-9 (92 kD), pro-MMP-2 (68 kD), and active MMP-2 (62kDa). The arrow on the left show the proteolytic activity associated with plasmin. (B) The active/pro-MMP-2 ratio in vitreous samples from rabbits after injections of 0.05, 0.25, and 0.5 IU of plasmin. Data were calculated by dividing the density of the band for the active form by the density of the band for the latent form. The active/pro-MMP-2 ratios for the 0.25 and 0.5 IU injections were significantly higher than that of the control (*$P < .05$). MMP-2 = matrix metalloproteinase-2; MMP-9 = matrix metalloproteinase-9.

monoclonal antibodies against MT1-MMP diluted 200X (Daiichi Fine Chemical Co, Ltd, Toyama, Japan). After incubation with the antibodies, they were reacted for 30 minutes at room temperature with goat antibodies against mouse immunoglobulins conjugated to a peroxidase-labeled dextran polymer (En Vision+, Dako, Hamburg, Germany).[16] For a negative control, adjacent sections were processed by replacing the primary antibody with mouse IgG1 diluted 100X (Dako, Hamburg, Germany). Color was

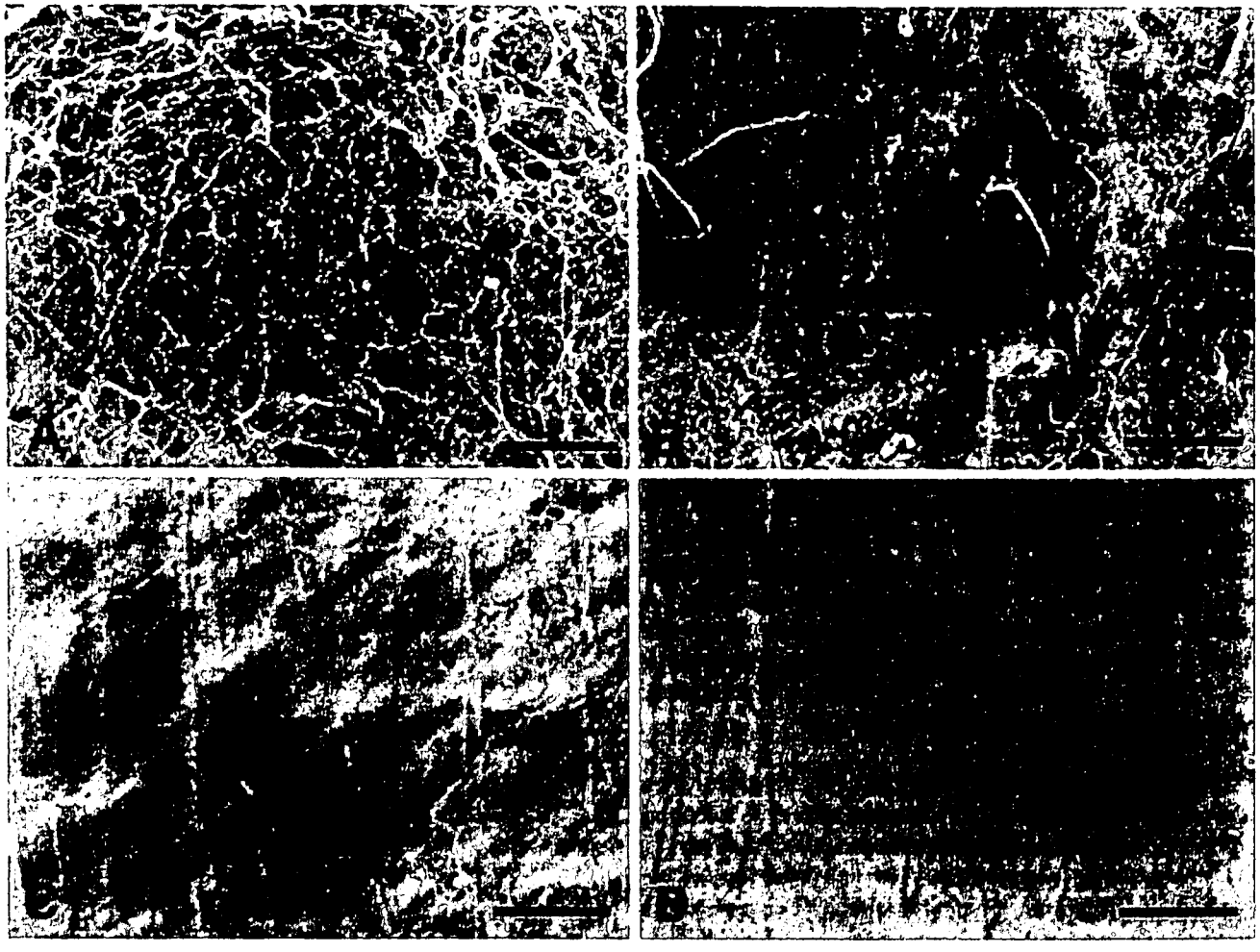

FIGURE 2. Scanning electron micrographs of the rabbit retinal surface 30 minutes after BSS or plasmin administration. (A) BSS injection. (B) 0.05 IU plasmin injection. (C) 0.25 IU plasmin injection. (D) 0.5 IU plasmin injection. Plasmin-treated eyes exhibited a smooth retinal surface that was dose-dependent. BSS = balanced salt solution; scale bars = 50 μm.

developed with 3, 3′-diaminobenzidine tetrahydrochloride. Sections of the negative control were counterstained with hematoxylin.

• MMP-2 ACTIVITY FOR HUMAN VITREOUS SAMPLES: To examine the activation ratio of MMP-2 in clinical cases, five human vitreous samples were analyzed by gelatin zymography. The patients in this study ranged in age from 57 years to 81 years. Two were female and three were male. All eyes had macular holes without PVD. Informed consent was obtained from all of the patients and the research adhered to the tenets of the Declaration of Helsinki. Ethical approval was obtained from the Human Studies Committee of Kumamoto University. After anesthesia, we started pars plana vitrectomy without any infusion and an undiluted vitreous sample of approximately 0.3 ml was collected in a syringe connected to the vitreous cutter. A pars plana injection of 0.5 IU of autologous plasmin into the vitreous cavity was performed using a 30-G needle. Fifteen minutes later, vitrectomy was restarted and a vitreous sample of approximately 0.3 ml was collected. The samples were stored in the same way as those obtained in the rabbit experiments.

• STATISTICAL MEASUREMENT: To compare the activation ratio of MMP-2 in vitreous samples after the injection of the various doses of plasmin and the time course of MMP-2 activity after plasmin administration, data were evaluated by means of analysis of variance (ANOVA), with a Fisher PLSD test or Scheffé F-test used for multiple comparisons. Values of the activation ratio of MMP-2 before and after the injections of plasmin in human vitreous were analyzed by a paired t test. Differences were considered to be significant when $P < .05$.

RESULTS

• DOSE EFFECTS OF PLASMIN ON MMP-2 ACTIVITY: To examine the dose effects of plasmin on MMP-2 activity,

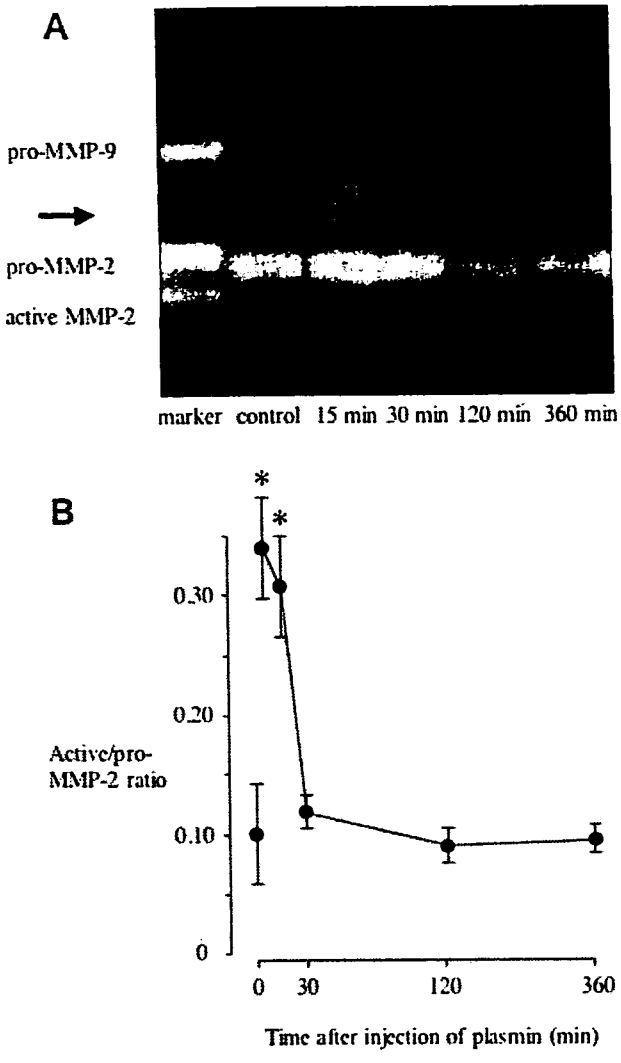

FIGURE 3. (A) Gelatin zymography of the vitreous samples from rabbits at 15, 30, 120, or 360 minutes after the injection of 0.5 IU of plasmin. The activity is visualized as the clear band, the positive markers indicate pro-MMP-9 (92 kD), pro-MMP-2 (68 kD), and active MMP-2 (62 kDa). The arrow on the left show the proteolytic activity associated with plasmin. (B) The active/pro-MMP-2 ratio in vitreous samples from rabbits at 5, 15, 30, 120, or 360 minutes after the injection of 0.5 IU of plasmin. Data were calculated by dividing the density of the band for the active form by the density of the band for the latent form. At 5 and 15 minutes after the plasmin injection there was a significant difference from the control values (*$P <$ .05). MMP-2 = matrix metalloproteinase-2; MMP-9 = matrix metalloproteinase-9.

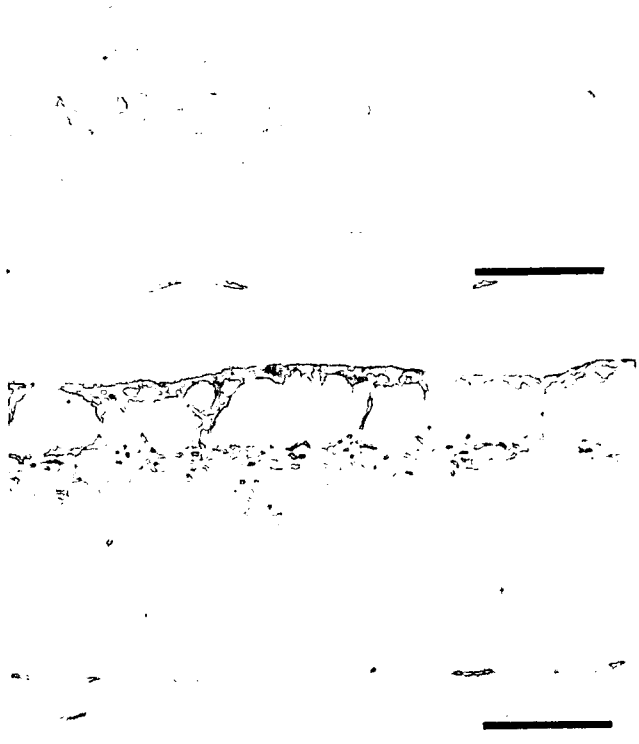

FIGURE 4. Immunohistochemical localization of MT1-MMP on the rabbit retina. Protein expression was detected with 3, 3' -diaminobenzidine tetrahydrochloride. (Top) For a negative control, the primary antibody was replaced with mouse IgG1 in an adjacent section and it was counterstained with hematoxylin. (Bottom) Serial sections were immunostained with monoclonal antibodies against MT1-MMP. MT1-MMP expression can be observed at the inner retinal layer. MT1-MMP = membrane-type 1 matrix metalloproteinase. scale bars = 50 μm.

vitreous samples were analyzed by gelatin zymography. MMP-2 was identified as the clear bands within the gels (Figure 1A). By using comparisons to the positive markers for pro-MMP-9 (92 kD), pro-MMP-2 (68 kD), and active MMP-2 (62kDa), we were able to detect the gelatinolytic 68 kD band of pro-MMP-2 and the 62 kD band of active MMP-2 in all of the vitreous samples. In this experiment, there was no evidence of presence and/or activation of MMP-9 in the examined vitreous samples.

Densitometric analysis of the bands revealed that the active/pro-MMP-2 ratio in the control was 0.10 ± 0.04 (n = 4), and the active/pro-MMP-2 ratio in the vitreous after the injections of 0.05, 0.25, and 0.5 IU of plasmin were 0.20 ± 0.06 (n = 4), 0.27 ± 0.05 (n = 4), and 0.30 ± 0.03 (n = 4), respectively (Figure 1B). There was a significant difference among groups with the values for the active/pro-MMP-2 ratios after the 0.25 and 0.5 IU plasmin administrations found to be especially significantly higher as compared with that seen for the control (P = .0032, P = .0025, respectively) (Figure 1B).

• SCANNING ELECTRON MICROSCOPY: Figure 2 shows an example of the retinal surface observed by SEM. For controls, whole areas of the retinal surface were covered with

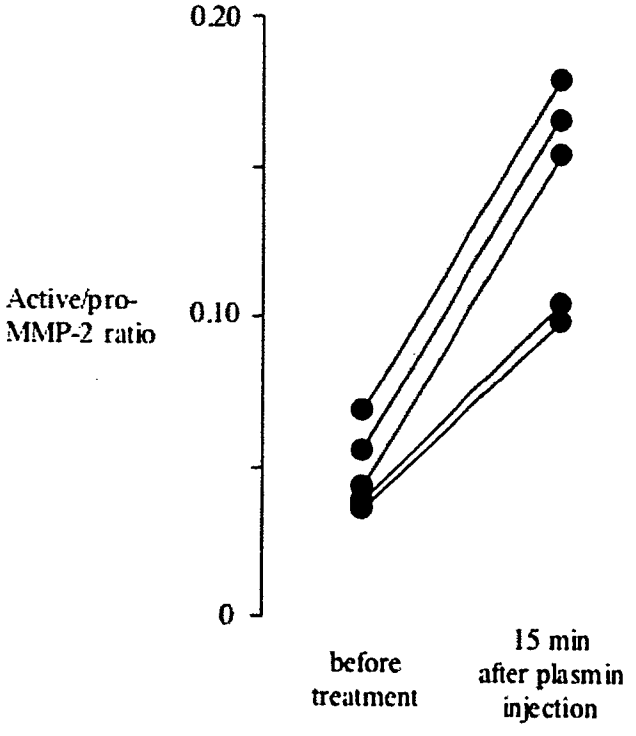

FIGURE 5. The active/pro-MMP-2 ratio in vitreous samples from five patients with macular holes. Vitreous samples were obtained before and 15 minutes after the injection of 0.5 IU autologous plasmin. The active/pro-MMP-2 ratio after the plasmin injection was significantly higher than the ratio observed before the plasmin injection ($P < .05$). MMP-2 = matrix metalloproteinase-2.

a fine collagenous material, which corresponded to the vitreous fibers (Figure 2A). These vitreous fibers were attached to the retina, especially in the region of the medullary rays. The retinas treated with 0.05 IU of plasmin still showed numerous vitreous fibers that covered the retinal surface (Figure 2B). In contrast, the retinas in the groups treated with 0.25 or 0.5 IU of plasmin exhibited smooth surfaces without any remnant of vitreous fibers except in the areas of the medullary rays (Figures 2C and D).

• TIME COURSE EFFECTS OF MMP-2 ACTIVITY AFTER PLASMIN ADMINISTRATION: To evaluate the time course effects of MMP-2 activity after plasmin administration, vitreous samples were analyzed by gelatin zymography (Figure 3A). As determined by densitometric analysis, the active/pro-MMP-2 ratio in the control vitreous was 0.10 ± 0.04 (n = 4), while the active/pro-MMP-2 ratios in the vitreous at 5, 15, 30, 120, or 360 minutes after the injection of 0.5 IU of plasmin were 0.33 ± 0.05 (n = 4), 0.30 ± 0.03 (n = 4), 0.12 ± 0.01 (n = 4), 0.09 ± 0.01 (n = 4) and 0.10 ± 0.01 (n = 4), respectively (Figure 3B). At 5 and 15 minutes after the plasmin injection, there was a significant difference from the control data ($P < .0001$). Additionally, there was also no evidence of presence and/or activation of MMP-9 in the examined vitreous samples.

• LOCALIZATION OF MT1-MMP: To detect tissue localization of MT1-MMP, immunohistochemical staining was performed. No staining was observed with mouse IgG1, which was used as the negative control. MT1-MMP expression was shown at the cell surface in the rabbit retina, especially in the inner retinal layer (Figure 4).

• MMP-2 ACTIVITY AFTER ADMINISTRATION OF PLASMIN IN HUMAN VITREOUS CAVITY: To evaluate the activation ratio of MMP-2 in clinical cases, human vitreous samples were analyzed by gelatin zymography. In human vitreous samples, there was also no evidence of presence and/or activation of MMP-9. During the procedures for these five cases, PVD was induced in all patients with or without a combination of core vitrectomy. All of these patients showed closure of the macular hole after the surgery. The active/pro-MMP-2 ratio before autologous plasmin injection was 0.05 ± 0.01 (n = 5). After injection of 0.5 IU of plasmin, the active/pro-MMP-2 ratio increased significantly to 0.14 ± 0.04 ($P = .0013$, paired t test) (Figure 5).

DISCUSSION

IN THE PRESENT STUDY, WE MEASURED THE ACTIVE MMP-2 level after the injection of various doses of plasmin and demonstrated a dose-dependent increase of active MMP-2. The time course of MMP-2 activity after plasmin administration showed that the MMP-2 was significantly activated at 5 and 15 minutes after the injections and decreased rapidly thereafter, whereas our gelatin zymography did not indicate the presence and/or activation of MMP-9.

The amount of liquefied vitreous and the ratio of the posterior vitreous detachment increase with age.[22] There is also an age-related increase of plasmin(ogen) in human vitreous that may be responsible for the degenerative changes in the vitreous such as vitreous liquefaction and posterior vitreous detachment.[14] Pro-MMP-2 is efficiently activated in the fibrovascular tissue during proliferative diabetic retinopathy and probably occurs as a result of the interaction with MT1-MMP and the tissue inhibitor of metalloproteinase (TIMP)-2.[16] This activity of MMP-2 and MT1-MMP has been suggested to be involved in the formation of the fibrovascular tissues.[16] Brown and associates showed that experimentally injected active MMP-2 cleaves vitreous collagen and they concluded that MMP-2 activity thus could be considered to be a potential mechanism for the vitreous liquefaction that is seen in aging and various pathologic states.[13]

It has been shown that there is an immediate decrease in MMP-2 activity because of various endogenous MMP